ELSEVIER

Materials and Engineering B102 (2003) 403–408

MATERIALS SCIENCE & ENGINEERING B

www.elsevier.com/locate/mseb

Systematic positron study of hydrophilicity of the internal pore surface in ordered low-*k* silica thin films

R. Escobar Galindo [a,*], A. van Veen [a], H. Schut [a], S.W.H. Eijt [a], C.V. Falub [a], A.R. Balkenende [b], F.K. de Theije [b]

[a] *Interfaculty Reactor Institute, Delft University of Technology, Mekelweg 15, NL-2629 JB Delft, The Netherlands*
[b] *Philips Research Laboratories, Prof. Holstlaan 4, NL-5656 AA, Eindhoven, The Netherlands*

Abstract

Non-destructive Doppler Broadening (DB), Positronium fraction (*f-Ps*) and Two Dimensional Angular Correlation of Annihilation Radiation (2D-ACAR), Positron Beam Analysis (PBA) techniques have been used to study well-ordered mesoporous silica thin films with hydrophobic or hydrophilic character. The DB results, characterized by the *S* and *W* parameters, are related to both the open volume and the chemical environment at the positron annihilation site. The *f-Ps* and 2D-ACAR techniques are very sensitive probes to determine the type of porosity (open or closed in terms of positronium escape) in thin film materials. Samples with varying pore size (well-controlled at 2, 3 and 4.5 nm, or incorporating microporosity in the silica), pore fraction (from 4 to 57%) and extent of hydrophilicity have been studied. In the hydrophilic samples with small pore size the *S*-parameter increases with the porosity while the *Ps*-fraction remains almost unchanged. Increasing the pore size leads to smaller changes in *S* with increasing porosity. However, an abrupt change in the *Ps*-fraction is observed for samples with porosity higher than 45%, indicating a positronium percolation threshold for samples with 2D ordering structure. On the other hand, for hydrophobic samples with high porosity (57%) the highest *S* parameter and *Ps*-fraction were obtained for the three pore sizes studied. 2D-ACAR is used to determine the fraction and velocity of *Ps* escaping from some of the latter samples exhibiting positronium percolation. The relationship between these observations and porosity will be discussed in terms of branching of the positron annihilation channels inside the mesoporous films.

Keywords: Positrons; Annihilation; Silicon oxide; Surface composition; Percolation phenomena

1. Introduction

Materials with a low dielectric constant ($k < 2.2$) are desired for future generations of ICs, in order to substitute the present dielectric layers in Ultra Large Scale Integrated (ULSI) devices. Candidates include, e.g. organic and inorganic polymers, and nanoporous silica. A high porosity of the material is necessary to lower the dielectric constant sufficiently. Further, pore sizes should be small (typically < 5 nm) and the material should preferably be hydrophobe. This can be accomplished by modifying the composition of the internal pore surface, such that hydrophilic silanol groups are replaced by hydrophobic methyl groups.

One of the few techniques capable of probing the pore size and distribution in the nanometer scale is Positron Beam Analysis (PBA) [1,2]. Recent positron studies [3–5] on randomly ordered pores in low-*k* thin films have been made using Doppler Broadening and lifetime experiments. The aim of this work is to study the effect of the composition of the internal surface on Doppler Broadening and to use the high resolution of 2D-ACAR for reference measurements on a few selected samples. This completes previous PBA studies on low-*k* thin films with well-defined pores [6,7].

* Corresponding author. Tel.: +31-15-2781612; fax: +31-15-2786422.
E-mail address: rescobar@iri.tudelft.nl (R.E. Galindo).

0921-5107/03/$ - see front matter © 2003 Elsevier B.V. All rights reserved.
doi:10.1016/S0921-5107(03)00121-1

2. Experimental procedure

The mesoporous silica samples were produced using solutions containing silicon alkoxides (tetraethylorthosilicate (TEOS) and methyltrimethoxysilicate (MTMS), see Fig. 1) and a surfactant (cetyltrimethylammonium bromide (CTAB), Pluronic F127 (ethylene oxide)$_{106}$(propylene oxide)$_{70}$(ethylene oxide)$_{106}$, or Brij76 $(EO)_{10}C_{18}H_{37}$. During coating deposition the solvents evaporate, micelles are formed and the silicon alkoxide condenses to form (organically modified) silica around the micelles. A well-ordered pore structure is obtained once the micelles are removed from the coating [6]. A list of the samples studied and some of their properties are summarized in Table 1. The layer thickness and porosity (from the refractive index using a Bruggeman effective medium approximation) have been obtained from ellipsometry. The pores are highly uniform and form an ordered mesophase. The lattice constant perpendicular to the surface was determined using θ–2θ X-ray diffraction. From 2D XRD it is known that the TEOS/CTAB system forms a 3D hexagonal phase, while the TEOS/F127 system results in a 2D hexagonal packing of cylinders in the plane of the surface. The latter structure is also the most likely one for the other systems.

Layers based on TEOS exhibit an internal surface area which is rich in silanol groups, while MTMS mixed with TEOS results in a more hydrophobic surface due to the incorporation of methyl groups in the pore walls. A completely hydrophobic surface is obtained when the MTMS to TEOS ratio exceeds 1. An alternative way to introduce methyl groups is by reaction of trimethylchlorosilane (TMCS) with the silanol groups. In this way every reacting silanol group is replaced by three methyl groups (via a Si atom). Although the pores become very methyl rich, the reaction with silanol groups is incomplete and results in an intermediate hydrophobicity. Four sets of samples were studied:

1) Samples based on solutions containing TEOS and different amounts of CTAB. The porosity after curing corresponds to the volume fraction of CTAB in the deposited layer. Note that ordered pores are only present at the highest amounts of CTAB. For smaller CTAB volume fractions at least part of the CTAB will be present as individual molecules, leading to layers which are (in part) microporous. With higher CTAB content the pore diameter is about 2 nm (based on cross-sectional TEM) and the pores can be considered as spherical inclusions which form a 3D-hexagonal stacking. The films are hydrophilic as they contain silanol groups.
2) Samples based on TEOS solutions containing different amounts of F127 surfactants. At high F127 content their pore size is about 4.5 nm and the pores can be considered as cylindrical inclusions that form a 2D-hexagonal packing of rods lying flat in the surface plane. These films are also hydrophilic.
3) Highly porous samples based on MTMS-rich solutions (TEOS/MTMS = 1) containing different surfactants (CTAB, Brij76 (pore size $\sim$3 nm) or F127). The films are hydrophobic as they contain a sufficient amount of methyltrimethoxysilane (MTMS), leading to a pores surface covered with a methyl groups. The different surfactants are responsible for the difference in pore size. The Brij76 and F127 samples are 2D hexagonally ordered. On the basis of the high porosity and cross-sectional TEM it is assumed that the methyl-rich CTAB-sample is also 2D ordered.
4) Samples of intermediate hydrophobicity, containing CTAB as the surfactant. Prepared by: (a) adding a relatively small amount of MTMS to the solution; and (b) giving the film a posttreatment with the hydrophobic molecule TMCS.

The *PBA experiments* were performed with the Delft Variable Energy Positron beam (VEP) [8]. The positrons were injected in the samples with energies tuned between 100 eV and 30 keV. The maximum implantation energy corresponds to a typical implantation depth of $\sim$5 μm in materials with $\rho \sim 2$ g cm^{-3}. All experiments were carried out at room temperature under a vacuum of about 10^{-6} Pa. The obtained PBA results are presented in terms of three parameters (S, W and *f-Ps*) [1]. The S parameter indicates the contribution of positrons that annihilate with low momentum electrons (valence or conduction electrons). This parameter is related to the open volume defects present in the sample (e.g. pores). The W parameter indicates the fraction of positrons that annihilates with high momentum electrons (core electrons). This parameter is related to the chemical environment where the annihilation takes place. Both parameters can be combined in S-W maps where the different annihilation sites (layers) can be distinguished. The data was analysed with the VEPFIT [9] program. The third parameter (*f-Ps*) is related to the ortho-Positronium (*o-Ps*) self-annihilation (3γ annihilation). *f-Ps* correlates with the presence of large open volume

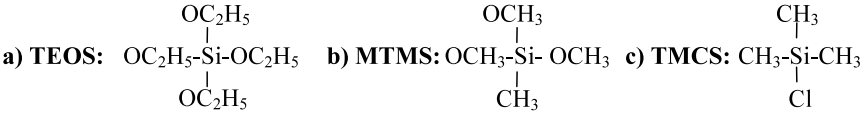

Fig. 1. Schematic representation of the molecules involved in the composition of the samples studied: (a) TEOS; (b) MTMS; and (c) TMCS.

Table 1
Description of the 4 series of low-k samples studied

Sample	Composition	Thickness (nm)	Porosity (%)	Pore size (nm)	Density (g cm^{-3})	Hydro-
1a	TEOS/CTAB = 0.01	184	11	1.0±0.5	2.0	-philic
1b	TEOS/CTAB = 0.05	267	31	1.0±0.5	1.5	-philic
1c	TEOS/CTAB = 0.1	338	46	1.75±0.25	1.2	-philic
2a	TEOS/F127 = 0.0005	190	7	1.0±0.5	2.0	-philic
2b	TEOS/F127 = 0.002	285	35	1.0±0.5	1.4	-philic
2c	TEOS/F127 = 0.005	457	45	4.5±0.5	1.2	-philic
3a	TEOS/MTMS = 1 CTAB 0.30	518	57	1.75±0.25	0.9	-phobic
3b	TEOS/MTMS = 1 Brij76 0.14	503	56	3.4±0.3	1.0	-phobic
3c	TEOS/MTMS = 1 F127 0.0064	1327	57	4.5±0.5	1.0	-phobic
4a	TEOS/MTMS = 3 CTAB 0.10	355	42	1.75±0.25	1.3	Partly-phobic
4b	TEOS/CTAB = 0.10 Grafted with TMCS	464	35	1.75±0.25	1.4	Partly-phobic

and it will be used here to characterise the presence of positronium percolation in the samples.

The 2D-ACAR method [10] measures the deviation, of the order of a few milliradians, from the collinearity between the two annihilation photons. A high-intensity (10^8 e^+/s) tunable keV positron beam POSH [11], which employs a reactor based positron source, has been recently coupled to the 2D-ACAR target and detection system, enabling depth-selective studies in the (sub)-μm range. 2D-ACAR is a sensitive probe for resolving para-Positronium (*p-Ps*) annihilation in nanoporous materials [12,13].

3. Results and discussion

The PBA results are summarized in Table 2 and plotted in Fig. 2. In [6] the PBA results of the hydrophilic samples (series 1 and 2) are discussed in terms of a 4-layer system (surface, low-k layer, substrate-interface and substrate). Here we will discuss the changes observed in the low-k layers due to variation in the composition of the internal surfaces, in the structural ordering, in the porosity and in the pore size.

In the TEOS-derived hydrophilic *CTAB* samples the S parameter associated with the low-k coating increases and the W parameter decreases linearly with porosity as can be seen in Fig. 2(I) and (II), respectively. The positronium fraction is negligible for these samples as can be seen in Fig. 2(III). The hydrophilic *F127* samples behave similar until 45% porosity is reached (2c). Then, the S parameter remains constant, the W parameter increases and the positronium fraction increases up to 0.48. This change in the *f-Ps* is related with the effusion of Positronium from the sample [7] and indicates a percolation threshold for positronium between 35 and 45% porosity in these samples, i.e. at the border between micropores and ordered mesopores.

The addition of MTMS enhances the effect of porosity: S increases and W decreases. This effect is most pronounced for the sample treated with TMCS, which leads to a high loading of methyl groups with the pores. The effusion of Ps is less clearly related to the methyl content of the layers. The most significant change occurs in methyl-rich samples with high porosity (3a, 3b and 3c) as the *f-Ps* increases up to $\sim$0.8, clearly indicating Ps flying-off the sample.

In terms of positron annihilation the porosity of the samples with low *f-Ps* is usually referred to as 'closed',

Table 2
VEPFIT analysis and fractions α and β from the branching scheme on the samples studied

Sample	Porosity (%)	$S_{coating}$	$W_{coating}$	f_{Ps} (3γ)	α (%)	β (%)
1a	11	0.954	1.64	0	11±1	100±10
1b	31	0.992	1.46	0.12	33±3	64±6
1c	46	1.010	1.40	0.12	44±4	73±7
2a	7	0.982	1.56	0	30±3	100±10
2b	35	0.994	1.40	0.08	36±4	78±8
2c	45	0.994	1.48	0.48	–	–
3a	57	1.060	1.28	0.8	–	–
3b	56	1.080	1.30	0.85	–	–
3c	57	1.070	1.30	0.85	–	–
4a	42	1.040	1.28	0.15	61± 6	76±8
4b	35	1.104	1.04	0.15	99±10	85±9

The typical error in S and W parameters affects the last significant digit.

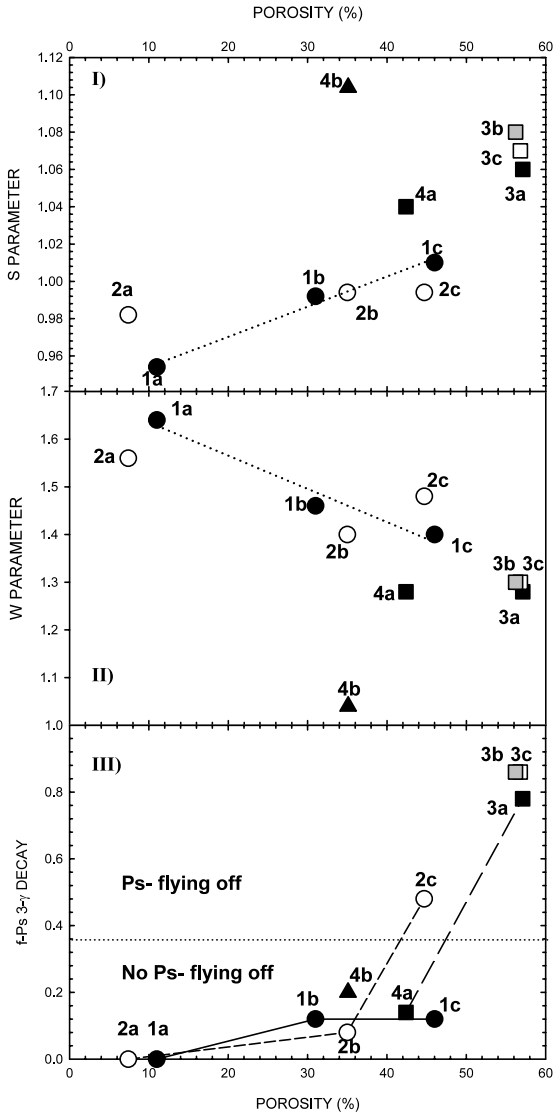

Fig. 2. Positron Beam analysis experimental results: (I) *S*-parameter; (II) *W*-parameter; and (III) Positronium fraction via 3γ decay (*f-Ps*) as a function of the porosity of the samples. The labels correspond to the sample description in Tables 1 and 2. The dotted lines in (I) and (II) indicate a linear relation between the *S* and *W* parameters and the porosity of the hydrophobic CTAB samples. The horizontal dotted line in (III) estimates the percolation threshold from changes in the *f-Ps* fraction in the samples.

implying that, within its limited lifetime, a positronium cannot escape from the layer any in significant amounts. However, it should be noted that this nomenclature does not mean necessarily that open porosity is absent. These layers are easily penetrated by gas molecules like water (e.g. evident from IR-spectroscopy) and N_2 or Kr (BET adsorption isotherm measurements yield a porosity that is in accordance with the porosity obtained from the refractive index).

A distinction can be made between samples with *f-Ps* values smaller than 0.3 and samples with *f-Ps* values higher than 0.4. The samples containing micropores (1a, 1b, 2a, 2b) all have a *f-Ps* value less then 0.15. Also the CTAB-derived samples which show a 3D hexagonal ordering (1c, 4a, 4b) have a low *Ps* fraction. The structure of the samples for which high *Ps* effusion is observed is a 2D hexagonal ordering of cylinders in the case of the F127 and Brij76 samples. The CTAB sample with high methyl content and 57% porosity (3a) is also likely to exhibit this type of ordering. Therefore we can estimate a positronium percolation threshold for the samples depending on the pore size, the porosity and the hydrophobic treatment. In Fig. 3 these observations are summarized, including an estimation of the positronium percolation threshold of the samples.

It is interesting to observe in Fig. 4 how plotting the *S* versus the *W* parameter for the different samples, all the CTAB samples without Ps effusion lay on a straight line towards higher *S* and lower *W* values. Only the sample 3a (*f-Ps* = 0.8) deviates from this behavior. Regarding the F127 and Brij76 series, it is observed that on three of the samples studied, 2c, 3b and 3c positronium percolation is detected. The *f-Ps* of those samples are 0.48, 0.85 and 0.85, respectively. Those samples also deviate from the *S*–*W* line of Fig. 4.

In order to investigate further the effect of Ps escaping from low-*k* dielectric thin films, sample 3c and 2c [7] were studied by depth-selective 2D-ACAR analysis. Table 3 presents data extracted from 2D-ACAR distributions measured for sample 3c at six positron implantation energies between 0.5 and 11 keV, corresponding to an average implantation depth range from 20 to 2 μm respectively. The spectra exhibit pronounced *off-centered p-Ps* peaks owing to the *p-Ps* atoms flying

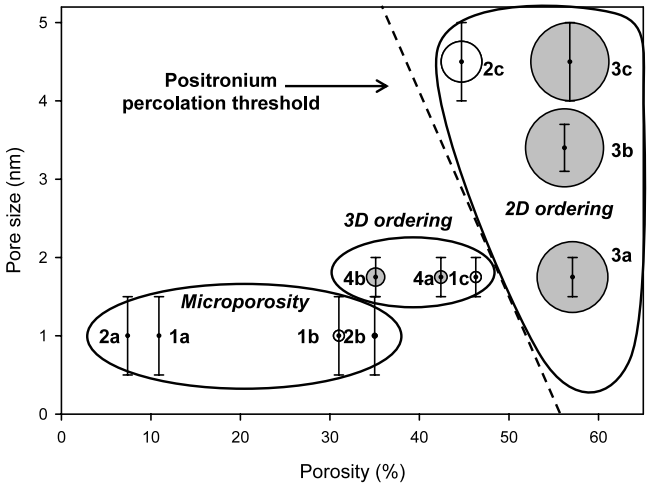

Fig. 3. Porosity versus pore size map for the low-*k* samples studied. The size of the circles scales to the *f-Ps* values of the samples. Open circles represent the hydrophilic samples and the closed circles represent the hydrophobic samples. The dotted line separates samples with positronium percolation from those without positronium percolation and gives an estimation of the percolation threshold dependence with pore size and porosity. Error bars on pore size are included according to values in Table 1.

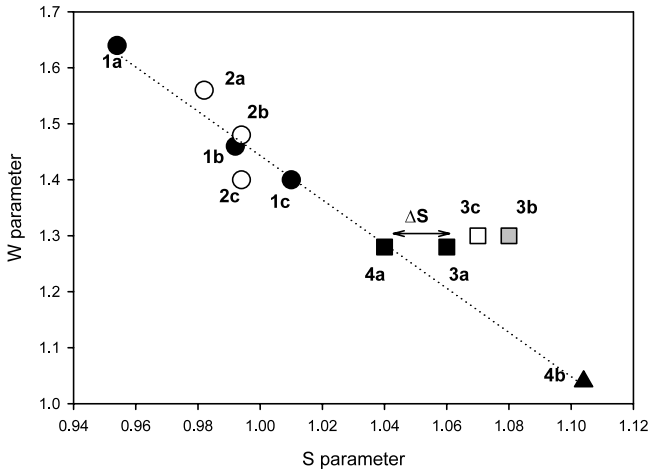

Fig. 4. S-W map with the VEPFIT results obtained for the low-k samples. The labels correspond to the sample description in Tables 1 and 2. The dotted line represents a linear fit of S versus W for the CTAB samples without open porosity. The change observed in sample 3a (ΔS) is related to Ps effusion.

off the sample into vacuum even at higher positron implantation energies [7]. The 2D-ACAR distributions were interpreted in terms of contributions from *p-Ps* flying off, a centered *p-Ps* component and a broad contribution from annihilation with amorphous silica. One observes that at 1.5, 3 and 5 keV the intensity of the total *p-Ps* (flying-off and annihilating in the low-k layer) remains fairly constant in agreement with the Doppler broadening measurements (S and 3γ) presented in [6]. This indicates a constant porosity throughout the low-k layer. The *p-Ps* is emitted from the low-k layer with an observed average velocity v_o (see Table 3). The velocity values decrease as function of depth, due to the increase of collisions with pore walls. This decrease clearly demonstrates that the *p-Ps* flying off is created deep inside the layer. For positrons implanted deeper into the sample the intensity of the flying-off component decreases as an increasing part of *Ps* atoms can not reach the outer surface within their finite average lifetime of 125 ps. The data is modeled in more detail in Ref. [14].

Apart from the effect on the *Ps* effusion fraction the S and W are very sensitive to the chemical groups present in the internal pore surface. The interaction of positrons with the hydrophobic groups produces strong effects on S and W as can be seen in Fig. 2(I) and (II). An increase of S and a decrease in W are observed in all those samples. Especially remarkable is the enormous increase in S on methyl-rich sample 4b, probably related to a higher *p-Ps* formation. Also the pick-off process of *o-Ps* might play a role in those changes.

The different processes involving positron implantation and Positronium formation and annihilation in systems that are closed with respect to positronium fly-off can be summarized in a branching scheme as shown in Fig. 5. According to this scheme the experimental S and W parameters related to 2γ events can be describe as follows:

$$S = k_{\text{bulk}} S_{\text{bulk}} + k_{\text{p-Ps}} S_{\text{p-Ps}} + k_{\text{pick-of}} S_{\text{o-Ps pick-off}} \quad (1a)$$

$$W = k_{\text{bulk}} W_{\text{bulk}} + k_{\text{p-Ps}} W_{\text{p-Ps}} + k_{\text{pick-off}} W_{\text{o-Ps pick-of}f} \quad (1b)$$

with the fractions of the different 2γ events,

$$k_{\text{bulk}} = \frac{1-\alpha}{1-\frac{3}{4}\alpha(1-\beta)}; \quad k_{\text{p-Ps}} = \frac{\frac{1}{4}\alpha}{1-\frac{3}{4}\alpha(1-\beta)};$$

$$k_{\text{pick-off}} = \frac{\frac{3}{4}\alpha\beta}{1-\frac{3}{4}\alpha(1-\beta)}$$

The *f-Ps* is related to 3γ events ($3/4\alpha(1-\beta)$) and therefore proportional to $\alpha(1-\beta)$ apart from a normalization factor. The determination of this factor depends on the measurement of a sample with 100% *o-Ps* self-annihilation as presented in [15] but for our qualitative disccusion we will omit this. As a first approximation we assume that the pick-off process is described with the same S and W parameters as the bulk annihilation [16]. Then, the experimental results can be interpreted in terms of α and β fractions (see Table 2). For example, the high value of S for sample 4b indicates an increase in the fraction of Ps formation inside the pores (α) towards values near 100%. So all positrons implanted in the samples will annihilate inside the pores as *Ps* for a porosity of 35%. This increase is completely different from the linear behaviour of α with porosity shown by the hydrophylic samples. The α linear behaviour is in

Table 3
Parameters of the 2D-ACAR fit for sample F127 3c

E_e^+ (keV)	Impl. depth (nm)	SiO_2	Flying p-Ps		Symmetric p-Ps	Si
		I (%)	I (%)	v_o ($10^{-3}c$)	I (%)	I (%)
0.5	20	87±5	9.0±2.0	2.10±0.10	4.0±2.0	0
1.5	80	80±4	13.0±2.5	1.90±0.10	7.0±2.5	0
3.5	300	80±3	7.0±0.1	1.65±0.10	13.0±1.5	0
5.0	550	77±7	1.5±2.0	1.50±0.15	16.5±1.5	5±5
8.0	1150	20±6	0.8±1.5	1.40±0.20	14.0±1.0	65±6
11.0	2000	5±5	0.3±1.0	1.35±0.25	4.0±0.5	90±5

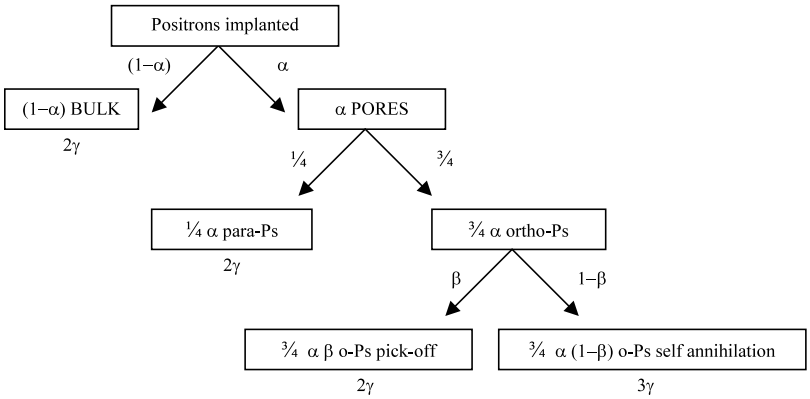

Fig. 5. Branching scheme of positron implantation, *Ps* formation and annihilation inside low-k dielectrics. The fraction of positrons annihilating as *Ps* inside the pores (α) is related to the porosity and the chemical composition of the internal pore surface of the pores. The *o-Ps* formation fraction is 3/4 of α. The fraction of *o-Ps* annihilated via pick-off (β) is related to the type of porosity and the chemical composition of the pores.

clear connection with the linear behaviour of S for the same hydrophilic samples as seen in Fig. 2. Further evidence on the anomalous α behaviour comes from the other intermediate hydrophobic sample (4a), which also allows the formation of *Ps* inside the pores to higher levels than the hydrophilic samples. Apparently, *Ps* formation by electron pick-up of positrons is relatively favourable in the case of pores containing a large amount of methyl groups.

An extension of this branching scheme to systems with open porosity together with the diffusion model presented in Ref. [6,14] will be presented in a future study.

4. Conclusions

PBA has been used to study differences between low-k dielectrics based on the pore size, the porosity and the composition of the internal pore surface. A positronium percolation threshold has been estimated based on *f-Ps* measurements. Samples with pore size of about 2 nm did not present percolation until 57% porosity is reached together with a hydrophobic MTMS addition. On samples with pore sizes of 4.5 nm, percolation is observed for lower porosity (45%) without any hydrophobic treatment. 2D-ACAR measurements were used to quantify the fractions and average velocities of flying-off *Ps* for one specific sample. The chemical composition of the internal surface pore is reflected in the changes observed on S and W parameters. Considering the proposed scheme of positron annihilation channels, these changes are related to an enhancement of *Ps* formation inside the pores decorated with methyl groups.

References

[1] A. van Veen, H. Schut, P.E. Mijnarends, in: P. Coleman (Ed.), Positron Beams and their Applications, World Scientific Publishing Co, 2000 (Chapter 6).
[2] H. Nakanishi, Y.C. Jean, in: D.M. Schrader, Y.C. Jean (Eds.), Positron and Positronium Chemistry, Studies in Physical and Theoretical Chemistry, vol. 57, Elsevier, Amsterdam, 1988, pp. 159–192.
[3] M.P. Petkov, M.H. Weber, K.G. Lynn, K.P. Rodbell, S.A. Cohen, J. Appl. Phys. 86 (1999) 3104–3109.
[4] K.P. Rodbell, M.P. Petkov, M.H. Weber, K.G. Lynn, W. Volksen, R.D. Miller, Mater. Sci. Forum. 363–365 (2000) 15–19.
[5] J. Sun, D.W Gidley, T.L. Dull, W.E. Frieze, A.F. Yee, E.T. Ryan, S. Lin, J. Wetzel, J. Appl. Phys. 89 (2001) 5138–5144.
[6] A. van Veen, R. Escobar Galindo, S.W.H. Eijt, C.V. Falub, H. Schut, A.R. Balkenende, F.K. de Theije, in these proceedings (E-I.2).
[7] R. Escobar Galindo S.W.H. Eijt, A. van Veen, H. Schut, C.V. Falub, IRI report IRI-Dm-2001-005 (2001).
[8] A. van Veen, J. Trace Microprobe Techniques 8 (1&2) (1990) 1–29.
[9] A. van Veen, H. Schut, J. de Vries, R.A. Hakvoort, M.R. Ijpma, In: P.J. Schultz, G.R. Massoumi, P.J. Simpson (Eds.), AIP 218, Positron Beams for Solids and surfaces, 1990, pp. 171–196.
[10] R.N. West, in: A. Dupasquier, A.P. Mills, Jr. (Eds.), Positron Spectroscopy of Solids, Proc. Int. School of Physics "Enrico Fermi" Course CXXV, IOS Press, Amsterdam, 1995, pp. 75–143.
[11] A. van Veen, H. Schut, J. de Roode, F. Labohm, C.V. Falub, S.W.H. Eijt, P.E. Mijnarends, Mater. Sci. Forum 363–365 (2000) 415–419.
[12] Th. Gessmann, M.P. Petkov, M.H. Weber, K.G. Lynn, K.P. Rodbell, P. Asoka-Kumar, W. Stoeffl, R.H. Howell, Mater. Sci. Forum 363–365 (2000) 585–587.
[13] S.W.H. Eijt, C.V. Falub, A. van Veen, H. Schut, P.E. Mijnarends, M.A. van Huis, A.V. Fedorov, Mat. Res. Soc. Symp.Proc. 647 (2001) O14.11.1-6.
[14] S.W.H. Eijt, A. van Veen, C.V. Falub, R. Escobar Galindo, H. Schut, P.E. Mijnarends, F.K. de Theije, A.R. Balkenende, Radiat. Phys. Chem. (2003) in press.
[15] H. Schut, R. Escobar Galindo, Z.I. Kolar, A. van Veen, G. Clet, Radiat. Phys. Chem. 58 (2000) 715–718.
[16] A. Alba Garcia, L.D.A. Siebbeles, A. Rivera, S.W.H. Eijt, R. Escobar Galindo, A. van Veen, Mater. Sci. Forum 363–365 (2000) 287–289.